doi:10.3788/gzxb20154405.0504002

用于反光电子谱可调带宽的紫外光子探测器

刘树虎[1],洪才浩[1],赵屹东[1],耿东平[2],郑雷[1],赵晓亮[1],李华鹏[1]

(1 中国科学院高能物理研究所,北京 100049)

(2 中国科学院上海应用物理研究所,上海 201800)

摘 要:设计并构造了一种用于反光电子能谱实验的窄带通真空紫外光子探测器,可以对能量在9.7 eV附近的光子进行计数.利用丙酮工作气体高通滤波与氟化锶窗口低能截止两种作用的叠加实现窄带通的效果.它的几何结构类似于一种特殊的盖革米勒型计数管,内部填充低气压丙酮和氩气混合气体,混合比例为1∶20.氟化锶作为入口窗,阻止大于9.7 eV的光子进入,而丙酮气用于捕获光子,使低能光子不能产生信号.利用氘灯光栅单色系统对窗口温度同带宽的关系进行了精确校定,使得探测器的光子能量带通宽度低于100 meV,并可以通过变化氟化锶窗的温度,使其可以被连续调整下降.温度控制系统的准确度可以达到±0.2 K.

关键词:探测器;光学带通;反光电发射;氟化锶;丙酮 ;温度控制;灵敏度;信噪比

中图分类号:O432.1;O582 **文献标识码**:A **文章编号**:1004-4213(2015)05-0504002-8

Tunable Narrow Bandpass Vacuum Ultraviolet Photon Detector for Inverse Photoemission Spectroscopy

LIU Shu-hu[1], HONG Cai-hao[1], ZHAO Yi-dong[1], GENG Dong-ping[1,2], ZHENG Lei[1], ZHAO Xiao-liang[1], LI Hua-peng[1]

(1 *Institute of High Energy Physics, Chinese Academy of Sciences, Beijing* 100049, *China*)

(2 *Shanghai Institute of Applied Physics, Chinese Academy of Sciences, Shanghai* 201800, *China*)

Abstract: This paper presents a novel Vacuum Ultraviolet (VUV) bandpass photon-counting detector which was designed to count photons with energies approximately 9.70 eV for inverse photoemission spectroscopy experiments. The performance was analyzed to improve the signal-to-noise ratio and resolution of the spectrum. The geometric structure of this detector is similar to a special Geiger-Müller tube. It is filled with a dilute mixture of acetone vapor and argon gas. The proportion was investigated and ascertained to be close to 1 to 20. A SrF_2 crystal was used as the input window to cut off high-energy photons with energies greater than 9.7 eV. Acetone vapor was selected as the functional gas to capture photons. Moreover, it can prevent low energy photons from being detected. The optical bandpass width is less than 100 meV and can be tuned continuously by cooling the SrF_2 window. The temperature is controlled by a self-developed cryogenic system with accuracy of±0.2 K. The relationship between the detector bandpass width and the SrF_2 window temperature is calibrated using a deuterium lamp and a grating monochromator.

Key words: Detector; Optical bandpass; Inverse photoemission; SrF_2; Acetone; Temperature control; Sensitivity; Signal to noise ratio

OCIS Codes: 040.5160 ; 040.7190; 120.4640; 230.0040; 300.2140

Foundation item: The National Natural Science Foundation of China (No. 11375227), The Instrument Developing Project of Chinese Academy of Sciences(No. 29201131231128010)

First author: LIU Shu-hu (1987-), male, Ph. D, mainly focuses on Synchrotron radiation optics and surface electronic structure of materials. Email:shliu@ihep.ac.cn

Supervisor(Contact author): HONG Cai-hao(1987-), male, research associate, P. H. D degree, mainly focuses on condensed materials, inverse photon emission spectroscopy and electronic optic simulation. Email:hongch@ihep.ac.cn

Received: Jan. 21, 2015; **Accepted**: Mar. 23, 2015

0 Introduction

Inverse Photoemission Spectroscopy (IPES) is the most direct technique to probe empty electronic states in solids and at surfaces. In an IPES experiment, a low energy electronic beam is utilized to inject into the unoccupied part of conduction band of solids. Then, the excited states will be de-excited to lower lying unoccupied final states, and vacuum ultraviolet photons will be emitted. Once injected electron energy is scanned with fixed special energy photons detected, the spectra of the energy band above the Femi level will be found. Unfortunately, IPE progress has an interactive cross section that is five orders of magnitude smaller than PE, as indicated by the low count rate in isochromat VUV detectors, which is a direct result of the poor Signal to Noise Ratio (SNR) of IPES. Moreover, PES has an energy resolution that is approximately 10 meV, far better than IPES, which has the highest resolution of approximately 200 meV. Currently, the development of IPES equipment shows that a high performance detector is the vital to the quality of the spectroscopic technique. Up to now, it is important to realize a high signal-to-noise ratio and narrow bandpass width VUV detector. In addition, those primary aspects, such as sensitivity, lifetime, dead time and background counts, are worthy of in-depth investigation. To be especially noted, the optical bandpass width is characterized by the Full Width at Half Maximum (FWHM) of the response function of the detector.

Ultraviolet photon detectors are used to record photons, which are emitted by electrons decaying from initial states to lower energy level states above the Fermi level E_f and have been under development for a long time[1]. These detectors may be divided into two types. One type can be called narrow bandpass detectors and commonly utilize fluoride crystals for cutoff[2], which generally occurs ~10 eV, to filter high energy photons. Electron generators with thin films or some gas are regarded as barriers to low energy photons entry[1].

These gas filling bandpass detectors employ the Geiger-Müller counter geometry structure, and they are originally used to capture Lyman-alpha radiation with iodine vapor. The electric field strength $\varepsilon(r)$ in this structure is proportional to the reciprocal of the radius $1/r$[3]. In this electric field, an avalanche would be formed when the initial ionization is caused. However, iodine vapor filling VUV detectors have a poor FWHMs and the count rate strongly depends on the temperature, i.e., 8%/℃[1].

The other type of detector detects photons using ay photomultiplier or Microchannel Plate (MCP) combination in a grating spectrometer[1]. Athough the later have a higher resolving power, the Geiger- Müller type bandpass detectors are more popular due to significantly lower costs compared with the grating spectrometers.

In fact, bandpass ultraviolet detectors can also be constructed without filling gas. N Sanada et al. took advantage of a CuBe electron multiplier with the first dynode as the photocathode to detect photons. However, comparisons of the two types bandpass detectors were performed, and the gas detector had a greater sensitivity than the solid-state-detector by a factor of 20[4]. All in all, Gas/window Geiger-Müller-type bandpass detectors are more popular.

CaF_2 is generally selected as the window for the bandpass detectors and has an energy cutoff at 10.08 eV, which results in an FWHM of approximately 300 meV for IPES combined with some filling gas at a mean energy 10 eV. By heating the CaF_2, the cutoff moves to lower energy. Thus, the FWHM can be changed to 130 meV. However, heating a CaF_2 window in an ultrahigh vacuum system is not a good idea for surface experiments. MgF_2 crystals with cutoffs at 10.97 eV have also been tried as the window of detector with different filling gases, similar to the CaF_2 detectors. Although the detector's mean energy has been improved by 0.8 eV, the FWHM of the MgF_2 detector is approximate 370 meV. This result is not better than the CaF_2 detector. We have to mention a double CaF_2 window detector, which achieved a FWHM of approximately 115 meV using krypton absorption lines[5]. This very exciting result significantly improved the resolution of the inverse photoemission spectrometer, but another two methods increase our expectations even more. One method is doping strontium into monocrystalline CaF_2, which achieves a FWHM of approximately 80 meV by mixing a suitable ratio of the three elements[6]. The other method is to cool a SrF_2 window to shift the cutoff toward higher energy. Using this method, an inverse photoemission spectrometer resolution of 165 meV was obtained.

However, the gases used to absorb ultraviolet photons played an important role in these detectors. Generally, acetone vapor and argon gas would be selected as the functional gases in a photon detector. The working gas acetone, which usually has a photoionization potential at approximate 9.7 eV acts a filter to prevent low energy photons from producing signals. Thus, only high energy photons are detected. Argon acts as a multiplier gas to form an avalanche, and adds significant amounts of negative charges to the amplifier input. Furthermore, the greater the charge,

the better the SNR. However, Ar^+ de-excitation and recombination with electrons at the surface of the cathode wall may produce ultraviolet photons, which can trigger an avalanche. Fortunately, acetone vapor is a kind of polyatomic molecular gas that is able to prevent the photon and ion feedback process.

We have constructed a double window Geiger-Müller type vacuum ultraviolet photon detector using SrF_2 crystals as the high energy cutoff and acetone as the filling gas. The cutoff energy of SrF_2 lies at approximately 9.7 eV, which is almost the same as the acetone ionization potential. It is took advantage of continuously adjustable FWHM by varying the temperature of SrF_2 window. The temperature range can be controlled from room condition to 210 ± 0.2 K at any point by a cryogenic system. The SrF_2 crystal was placed in an ultrahigh vacuum system. We focused on the realization of the SrF_2/acetone VUV detector and investigated the characteristics, to acquire a narrow bandpass width and a high signal to noise ratio.

1 Experiment

IPES is a complementary method to Photoemission Spectroscopy(PES) for mapping of the energy band structure across the Fermi level, as show in Fig. 1.

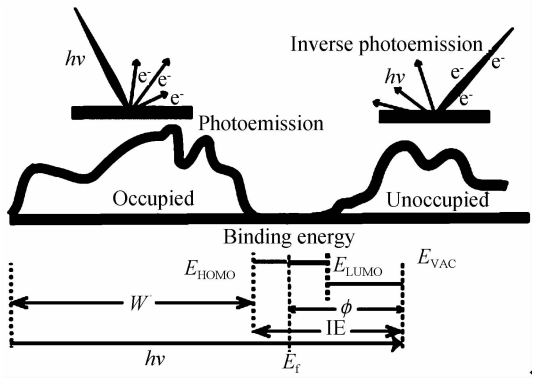

Fig. 1 The relationship between PES and IPES

Howeve, the performance of the detector determines the quality of the spectrum. A series of test and measurement systems were assembled for the characterization of the performance of the detector in Fig. 2.

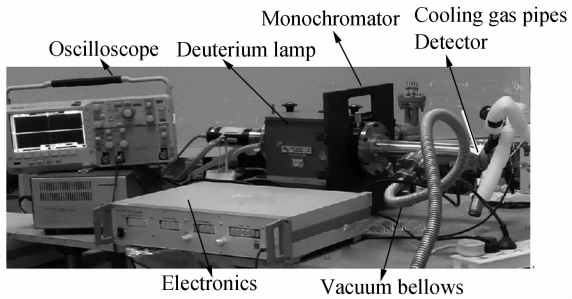

Fig. 2 Photograph of the measurement system

We employed a 150 W large power commercial deuterium lamp (L1835, Hamamatsu, Japan) as a photon source. It provides a stable output for a long time with extremely small fluctuation. A highly stable monochromator (VM-502, Princeton Instruments, USA) was arranged. Its single point resolution is 0.1 nm with sine bar-driven scanning system. The optical path was covered between them by nitrogen or extracted to a 10^{-2} Pa vacuum using a scroll pump.

The inflatable system of the detector was assembled under the vibration isolated optics table. It consists of stainless pipes, an Integral-Bonnet needle valve (Swagelok), a ceramic capacitor film absolute pressure transmitter (Shanghai Zhentai Instrument Co., Ltd.) and a turbo molecular pump unit (Edwards). High purity argon and liquid acetone with a purity of 99.5% were added to the system. The detector and system would be pumped to vacuum below 10^{-4} Pa. This step makes the detector more clear for filling functional gas and ionized electron multiplication. Then, liquid acetone was carefully added to the detector by a slowly rotating valve to vapor pressures between 100 Pa and 1500 Pa. Subsequently, Ar was filled into the detector so that the final pressure was in the region of 10 KPa. Both the acetone vapor and argon gas pressure were measured using a film absolute pressure transmitter. The gauge is resistant to corrosion from the acetone vapor. Its functional range was set to cover 0.2 Pa-26 KPa to obtain reliable and accurate measurements. However, it has to be calibrated when exposed to atmospheric pressure. Calibration can be performed in a vacuum system with a pressure below 0.13 Pa or 1×10^{-3} Torr. The electronics of the detector can supply the tungsten with anode voltages up to 1500 V and anode pulse signals are shaping-amplified by its amplifier with gain range from 1/2 to 20. All of the signals from the detector are shown on an oscilloscope (DPO2200B, Tektronix).

2 The realization of detector

The VUV detector geometric structure is similar to the end-window Geiger-Müller type counter as show in Fig. 3 where a is vacuum safe high voltage (SHV) feedthrough, b is hole punched for acetone vapor input, c is apertures of the cooling gas in and out, d is double sided CF flange, e is tungsten wire, f is 316L stainless-steel cathode cylinder, g is PTFE spacer, h is MgF_2 window, i is insulator PEEK, j is copper ring bracket, and k is SrF_2 window. It consists of an electropolished stainless steel cylindrical tube with an inner diameter of 27 mm welded to a double sided DN40 conflat flange. Two 3 mm diameter holes were punched to introduce cooling gas, and one hole with 1/4 inch in

diameter to fill functional gas to the detector. A tungsten wire anode with 1 mm diameter was placed at the center of cathode cylinder with a polytetrafluorethylene (PTFE) spacer. The spacer was added to the W wire approximately 70 mm from the front to keep the anode upright in the center and prevent it from vibrating. The double sided CF flange was sealed with a special vacuum safe high voltage feedthrough with a silicone ring to prevent corrosion from acetone vapor. A MgF_2 crystal with a thickness 2 mm and diameter of 26.5 mm with 90% transmittance at 9.7 eV was glued to the cathode tube inner using Torr Seal sealant epoxy. The distance between the tungsten cutting edge and the MgF_2 window is 5～10 mm. The lateral of MgF_2 window is a polyetheretherketone (PEEK) insulatorbracket. It was tightened to the outside of the cathode to fix oxygen-free copper, which was used to transfer heat between the cooling gas and SrF_2 window. A 316L stainless steel tube with a 3 mm outside diameter and 2 mm inner diameter was welded to the copper bracket with silver solder through double sided CF flange.

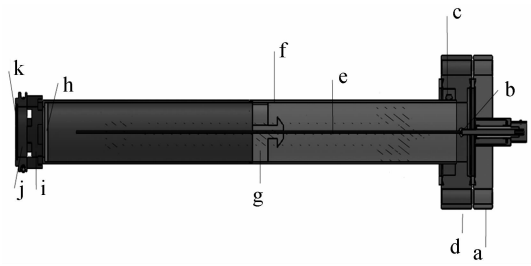

Fig. 3 Cross sectional design drawing of the VUV photon detector

Surfaces treatments are necessary for both the cathode inner wall and the anode tungsten wire. They all were ultrasonically cleaned in 65° warm water with metal cleaner for 90 minutes. Furthermore, they were washed with deionized water. The contact of the anode wire and the feedthrough must be specially insulated. The wire should be hand-polished on the frontier. Above all, the aim is to prevent ignition that always appears during research on this detector.

3 Results and discussion

3.1 Optical bandpass width

There is no doubt that FWHM estimated by the Full Width at Half Maximum is a significant characteristic of detector performance. The cutoff of the SrF_2 crystal had been measured at a vacuum ultraviolet photon beam station of the Beijing Synchrotron Radiation Facility (BSRF), China. A steep side is observed close to photon energy of 9.7 eV. The flux measurements at the front and back of the SrF_2 window do not occur at the same time, but are normalized by storage ring electron beam current, seen in Fig. 4.

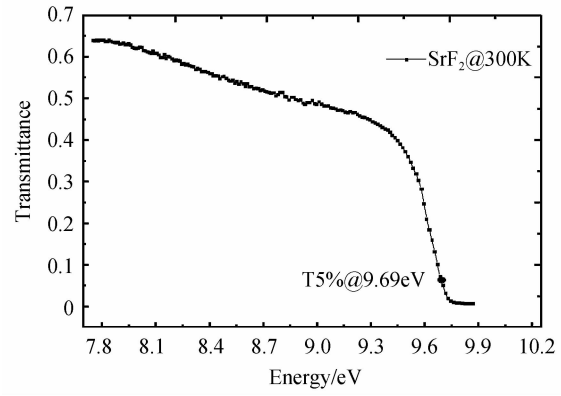

Fig. 4 Transmittance of the SrF_2 crystal window

Inco indicates that the transmittance of the SrF_2 crystal is only 5% at 9.69 eV under normal temperature conditions. As we all know, acetone photoionization threshold is also close to 9.69 eV, so the probability that the detector would create signals is extremely small. To expend the transmittance, cryogenic equipment was designed to reduce the temperature of the SrF_2 window, seen in Fig. 5 as showing the a compressed Nitrogen cylinder, b regulator, c screwed bonnet needle valve and pipe, d solenoid valve, e Dewar container, and f temperature controller. The high-energy cut-off position moved when its temperature is changed, and due to the photoexcitation of the crystal[20-21], higher energy photons are absorbed by the crystal.

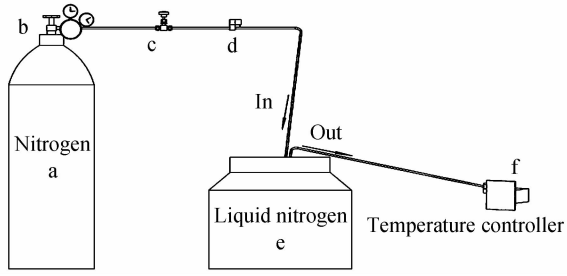

Fig. 5 Schematic of the cryogenic system for temperature control

A commercially available 13-MPa compressed nitrogen cylinder was used as the gas source to cool the crystal via the 6-mm diameter polyethylene tube connected by steel pipes with tube fittings. However, a Dewar with 77 K liquid nitrogen was added between the gas source and the cooled element. Using this method, normal nitrogen gas gets in and cryogenic gas goes out. Note must be mentioned is that the copper pipe should be set up for heat exchange between the nitrogen gas and liquid nitrogen. The key to keeping the window temperature stable at any point is to control the airflow, which is carried out using PI temperature controller and screwed bonnet needle valve.

The cooling extends the energy level slitting of the SrF_2, causing the SrF_2 cutoff to shift to higher energy level, although the resolution exhibits deteriorative trend (Fig. 6). The cutoff of the acetone vapor ionization is marked by a purple dash dot arrow. The optical bandpass width is measured using the FWHM (a). According variations in the bandpass width and count rate with the change of SrF_2 crystal window temperature is shown (b). The square point solid line represents the FWHM, and the count rate is indicated by the round point solid line.

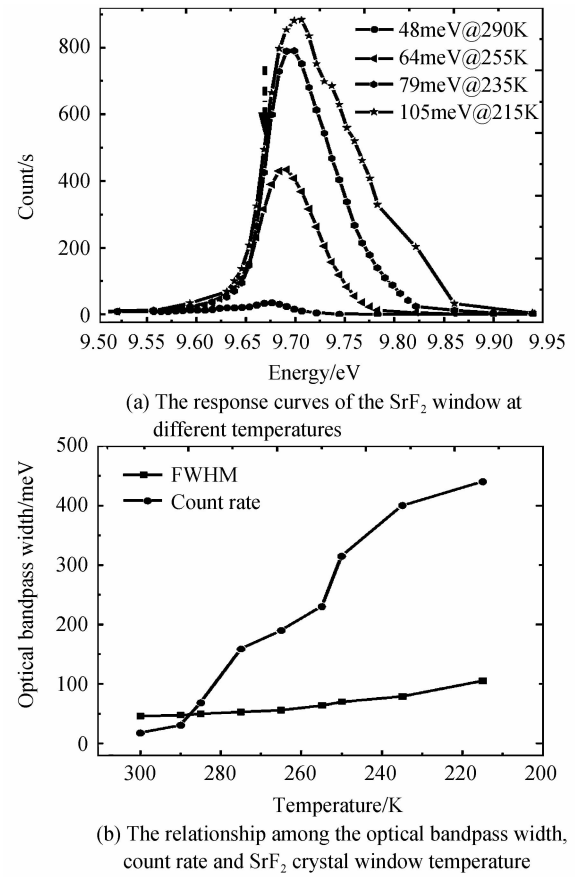

Fig. 6 Feature of SrF_2 crystal window

Obviously, the optical bandpass width can be adjusted continuously from 48 meV at room temperature to 105 meV after the SrF_2 is cooled to 215 K. In addition to the position of the high energy cutoff of the SrF_2 crystal, the other factor that contributes to the FWHM is acetone photoionization efficiency, which is impacted by gas-filled pressure and lower-lying acetone Rydberg states. The latter would be excited by photons with energies higher than the photoionization threshold together[22-23]. It is illustrated by the rising edges marked with the purple dash dot arrow in the Fig. 6 (a). For this reason, more researches should be conducted to obtain better FWHMs, and higher count rates.

In fact, the temperature of the SrF_2 window has a substantial impact on both the optical bandpass width and the count rate. The relationship among them was shown in Fig. 6(b). The lines show the corresponding variation of the count rate and bandpass width of the detector as the temperature of the crystal reduced. The optical bandpass width is confirmed using the FWHM and count rate is accessed from the partly peak position of response curve as schematized in Fig. 6 (a). Comparing the two solid curves, the optical bandpass width exhibits slower growth than the count. Moreover, this comparison sharply indicates that a decrease in the FWHM deterioration can rapidly upgrade the count rate of the detector, which improves the SNR. It is considerably significant for inverse photoemission experiment with different samples. Simply put, different samples would produce different photon signal intensities, then, the optical bandpass width and SNR have to be adjusted to adapt it.

The FWHM impacted by deuterium lamp had also been calibrated, because the deuterium light source possesses different photon fluxs as energy changed. A silicon photodiode solid detector (AUX-100G, IRD, USA) was selected to measure the monochromatic deuterium spectrum. Whereas the sensitivity of the solid detector is much lower than the gas detector, the slit width of the monochromator had to be larger than the previous optical design. The result shows that the morphology of response curve is unchanged, but the FWHM is found to be smaller by 10 meV, as show in Fig. 7.

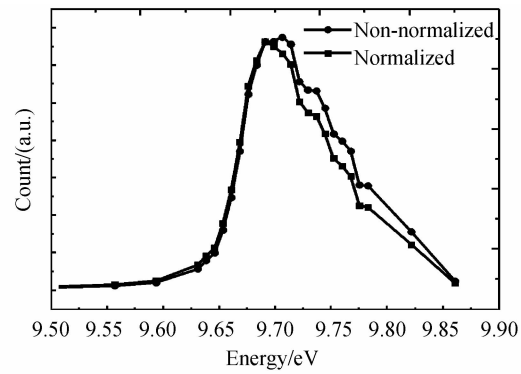

Fig. 7 The response of the detector normalized by the deuterium lamp spectrum

3.2 Sensitivity

However, besides the optical bandpass width, the sensitivity of the VUV photon detector is an important characteristic. It represents the ability of the detector to capture the photons and produce signals for recording. A higher transmittance and an optimized mixing argon to acetone vapor ratio, result in more photons in the beam being counted. As referred above, the transmittance of the window can be improved by reducing the SrF_2 temperature. To acquire superior sensitivity, the gas ratio is comprehensively studied

over a wide range.

The argon pressure was studied starting at 5 KPa. It is an extremely low atmosphere condition for acquiring sufficiently reliable signals with accommodative SNR. When the pressure promoted to greater than 15 KPa, no pulse could be observed, not even the cosmic background signals, despite an anode bias of 1500 Volts, which is the limit of our electronics. It is worth noting that acetone employed during the measurement was 300 Pa. As the same as argon, the acetone gas pressure was tested from 100 Pa to 1500 Pa. Of course, the argon would be filled into detector after the aceton with the mixed gas pressure eventually reaching approximately 10 KPa. The results are shown in Fig. 8. SrF_2 is cooled to 250 K for all of the conditions, and the significant changes are illustrated by the purple dash dot arrow. The colors and symbols are used to identify the different curves.

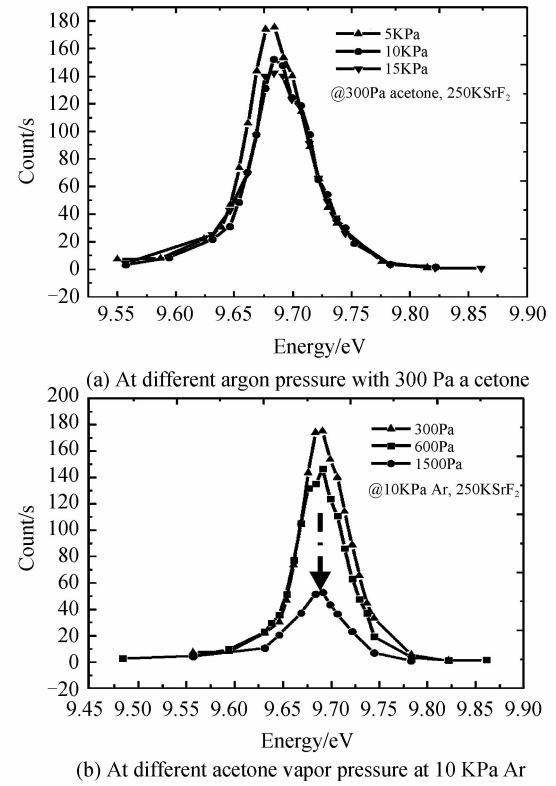

Fig. 8 Response curves of the detector

The argon gas pressure contributes a smaller impact than the acetone vapor on the count, as shown in Fig. 8(a). A pressure of 10 KPa argon obtains 30% count rate increment than 5 KPa in the peak position. The count is consistent when taking into account the experimental uncertainty. However, the detector exhibits greater sensitivity to the acetone vapor. Fig. 8 (b) shows that acetone at 300 Pa pressure produces three times as many count rate as at 1 500 Pa. It is an excellent explanation that acetone molecules play a quenching gas role as well as detection gas. Acetone is a polyatomic organic molecule that possesses a large of number non-radiative excited states, such as rotational and vibrational states, and capture the VUV range photons by dissociating. However, considering the voltage applied to anode and the detector lifetime, 300 ~600 Pa acetone vapor mixed with 10 KPa argon is found to be the best combination.

3.3 Dead time

The dead time is a symbol to reflect the count capacity of the detector. As others researchers have noted[24], the detector does not operate in the Geiger region, and the amplitude of the pulse signals showed considerable gaps among them. Fig. 9(a) was acquired by recording signal pulses for a relative long time with the oscilloscope, and the region of sparse pulses shows the distribution of the amplitudes, yet. Every pulse is represented by a black vertical line in the figure. The small illustration is the morphology of a single pulse. It is a significant information to discuss the inclusion of dead time in the recovery time. In a general Geiger-Müller-type counter, the threshold selects the pulses to be counted. The recovery time is determined by the time length between the pulses amplitude equal to the low threshold and up to the normal height. Thus, only the low count limit changed, and the recovery time would be extended or shortened accordingly. However, the variation in the pulse amplitude of the VUV detector is random without the condition of a high pulse followed by gradually increasing low pulses as in the general G-M counter. The space charge effect and photons entering at different transverse positions of the detector contribute to the phenomena. Here, the recovery time is not a meaningful and exact statement that reflects the response time of the detector. We fully believe that defining the pulse width as the dead time is reasonable, i. e. no counts occur, although photons may enter into the detector during this time. Consequently, the detector with long dead time is confirmed to suffer poor sensitivity. Our detector dead time was measured to be around 20 ~ 50 μs. This measurement was made under the detector low count frequency condition, which eliminates the influence of signal superposition. By this, the count frequency of the detector was estimated to be greater than 20 thousand per second. However, as shown in Fig. 9(a), an excessively high pulse frequency leads to low pulse amplitudes. The efficiency maximum count rate of the detector was evaluated to be not less than 5 thousand per second. For the IPES experiment, this circumstance demonstrates an adequately good SNR.

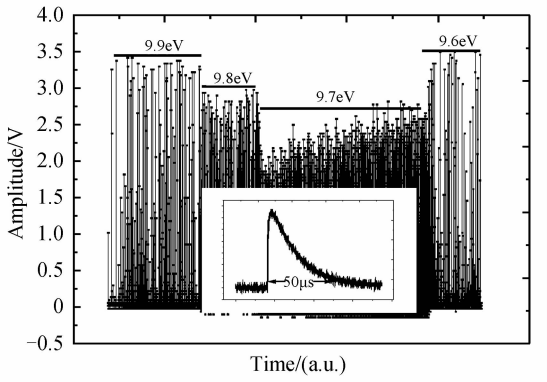

(a) The relationship between the photon energy and the pulses amplitude. The inset shows the width of the signal pulse

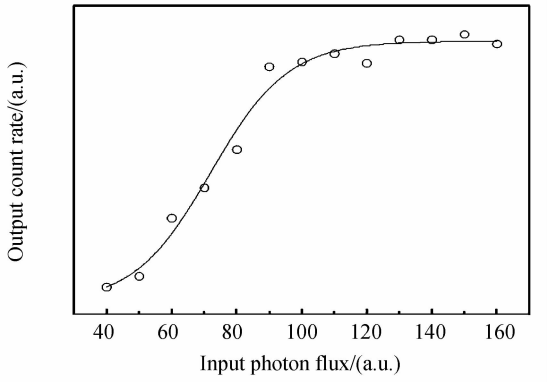

(b) The detector response capability curve

Fig. 9 The output feature

Interestingly, the oscilloscope was performed to record signals amplitudes for a long time as the energy changed from 9.9eV to 9.6eV. The observed amplitudes would be reduced in the higher count rate region but increased in the lower count rate region.

This behavior is similar to that observed in general count detectors. A more clear association is shown by the relative count capability of the detector. As shown in Fig. 9(a), the transmittance of SrF_2 is different for special energy photons, which are applied to gradually increase the input photon flux to the detector. However, the energy range is only around 0.3 eV. Within a certain range, the output rate of the detector and input photon flux have a nearly linear relationship. After that, the increased input photon flux cannot promote output count rate, as shown in Fig. 9(b). This result is represented by the hollow dots and the red line, which is the curve fitted with the Boltzmann function. Then, the detector is surmised to be saturated. Moreover, the electronics of the detector is excluded because of its 200 MHz count frequency. It is proved that the detector should be performed in a reasonable count rate range.

3.4 Background signals

The analysis of the source of the background signals to exclude false counts is performed. This analysis was performed using a scintillator detector system (Fig. 10). Cosmic energetic particles radiate earth with one per square centimeter per second. Both argon and acetone are ionized by them. Moreover, the impact of cosmic radiation on the inner wall of the detector also has a chance to create ultraviolet photons. Two scintillator detectors were placed on the top and bottom sides of the VUV detector. They were manipulated to monitor the coupling signals from the RIGOL four-channel digital oscilloscope after high-energy cosmic particles travel through them. These three detectors were placed in parallel with the ground. As the same time, the positive anode bias of the VUV detector would be varied to try to access the signal pulses. In addition, the low threshold of the detector is set much higher than the electronic noise, which can exclude the interference from electronics equipment and electric power fluctuations.

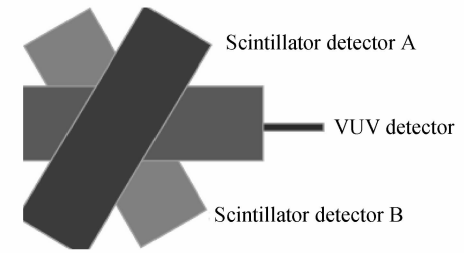

Fig. 10 Schematic diagram of the scintillator system

This calibration for the cosmic radiation background reveals an expected result. The count rate is less than 0.3 counts/s in the VUV detector when the scintillator detector coupling signal occurred, while the VUV detector channel collected many pulse signals because the baseline of oscilloscope had substantial jitter, although no coupled signals appeared. The jitter is regarded as ignitions occasionally and the appearance of the pulse is different from a true signal pulse. These results signify that the detector has low noise.

3.5 Lifetime

The lifetime is affected by many factors, such as the gas purity and laboratory light. They all cause the acetone molecules to dissociate. Although Maniraj M et al. tried to perform the measurement experiments of acetone detector using the synchrotron light source, much more extra works has to be conducted on the reduction of the intensity of light, taking into account the lifetime of the gas detector. The count rate decreased rapidly as the gas was depleted. However, the acetone partial pressure plays the most important role on the lifetime. The detector was continuously irradiated for 5 hours with 100 count/s, and no significant variations were discovered. However, the counting ability of the detector was lost after four months without use. This result could be explained by vacuum reduction, air infiltration changes the

atmosphere in our detector.

4 Conclusion

An extremely narrow optical bandpass width and highly sensitive Geiger-Müller-type VUV photon detector is realized. By cooling the SrF_2 input window, its FWHM can be continuously tuned from approximately 50 meV to 100 meV. Acetone vapor at 600 Pa mixed with 10 KPa argon and around 1000 V bias is determined to be the most appropriate combination for a high signal-to-noise ratio detector. Its dead time is only microseconds, which provides the detector with the ability to count thousands of photons per second. The background signal counts are lower than 0.3 counts/s, and a lifetime analysis was conducted to determine the actual count capability of the detector. The relationship between the SrF_2 window temperature and the optical bandpass width is described. The results make significant contributions to the surprising inverse photoemission spectroscopy in special experiments. Meanwhile, studies of VUV photon detectors do not need to be performed in ultrahigh vacuum spectrometer systems, and synchrotron light may be replaced by a deuterium lamp. This progress prominently simplifies the requirements to develop the equipment.

References

[1] PENDRY J. New probe for unoccupied bands at surfaces[J]. *Physical Review Letters*, 1980, **45**(16): 1356-1358.

[2] FUNNEMANN D, MERA H. 10 eV photon detector for inverse photoemission[J]. *Review of Scientific Instruments*, 1986, **19**(7): 554-447.

[3] BUDKE M, RENKEN V, LIEBL H, *et al*. Inverse photoemission with energy resolution better than 200 meV[J]. *Review of Scientific Instruments*, 2007, **78**(8): 083903.

[4] MANIRAJ M, D'SOUZA S W, BARMAN S R, *et al*. Photon detector for inverse photoemission spectroscopy with improved energy resolution[J]. *AIP Conference Proceedings*, 1349, **497**(2011), 2011: 497-498.

[5] BRACKMANN R T, FITE W L, HAGEN K E. Iodine-vapor-filled ultraviolet photon counter[J]. *Review of Scientific Instruments*, 1958, **29**(2): 125-128.

[6] SANADA N, SHIMOMURA M, FUKUDA Y. Inverse photoemission spectrometer using a BaF2 window for a low-pass filter[J]. *Review of Scientific Instruments*, 1993, **64**(12): 3480-3481.

[7] SCHÄFER I, DRUBE W, SCHLÜTER M, *et al*. Bandpass photon detector with high efficiency for inverse photoemission spectroscopy[J]. *Review of Scientific Instruments*, 1987, **58**(4): 710-711.

[8] AVCI R, CAI Q, LAPEYRE G J. Measurement of the absolute spectral response of an inverse photoemission detector [J]. *Review of Scientific Instruments*, 1989, **60**(12): 3643-3646.

[9] YOKOYAMA K, NISHIHARA K, MIMURA K, *et al*. Bandpass photon detector for inverse photoemission spectroscopy[J]. *Review of Scientific Instruments*, 1993, **64**(1): 87-90.

[10] LIPTON-DUFFIN J A, MARK A G, MCLEAN A B. Photon detection with n-propanol and C[sub 2]H[sub 6]O isomers[J]. *Review of Scientific Instruments*, 2002, **73**(9): 3149-3154.

[11] PRINCE K C. Improved inverse photoemission detector[J]. *Review of Scientific Instruments*, 1988, **59**(5): 741-742.

[12] CANTONI M, BERTACCO R. High efficiency apparatus for spin polarized inverse photoemission [J]. *Review of Scientific Instruments*, 2004, **75**(7): 2387-2392.

[13] DENNINGER G, DOSE V, SCHEIDT H. A VUV Isochromat Spectrometer for SurfaceAnalysis[J]. *Applied Physics* 1979, **18**: 375-380.

[14] DOSE V, MEYER V, SALZMANN M. Collisional quenching of metastable hydrogen[J]. *Journal of Physics B: Atomic and Molecular Physics*, 1969, **2**(12): 926-932.

[15] YOSHIDA H. Low-energy inverse photoemission spectroscopy using a high-resolution grating spectrometer in the near ultraviolet range [J]. *Review of Scientific Instruments*, 2013, **84**(10): 103901.

[16] FAUSTER T, STRAUB D, DONELON J J, *et al*. Normal-incidence grating spectrograph with large acceptance for inverse photoemission[J]. *Review of Scientific Instruments*, 1985, **56**(6): 1212-1214.

[17] HILL I G, MCLEAN A B. A comparison of two high performance inverse photoemission bandpass detectors[J]. *Review of Scientific Instruments*, 1998, **69**(1): 261-264.

[18] STIEPEL R, OSTENDORF R, BENESCH C, *et al*. Vacuum ultraviolet photon detector with improved resolution for inverse photoemission spectroscopy[J]. *Review of Scientific Instruments*, 2005, **76**(6): 063109.

[19] MANIRAJ M, D'SOUZA S W, NAYAK J, *et al*. High energy resolution bandpass photon detector for inverse photoemission spectroscopy [J]. *Review of Scientific Instruments*, 2011, **82**(9): 093901.

[20] HUNTER W R, MALO S A. The temperature dependence of the short wavelength transmittance limit of vacuum ultraviolet window materials-Ⅰ Experiment[J]. *Journal of Physics and Chemistry of Solids*, 1969, **30**(12): 2739-2745.

[21] MICHAEL H R. Temperature dependence of the short wavelength transmittance limit of vacuum ultraviolet window materials-Ⅱ Theoretical, Including interpretations for U. V. spectra of SiO_2, Ge2, and Al_2O_3[J]. *Journal of Physics and Chemistry of Solids*, 1970, **31**: 1041-1056.

[22] KIM J H, KANG D W, HONG Y J, *et al*. Ionization energy of acetone by vacuum ultraviolet mass-analyzed threshold ionization spectrometry[J]. *Hyperfine Interactions*, 2013, **216**(1): 85-88.

[23] WEI Li-xia, YANG Bin, WANG Jing, *et al*. Vacuum ultraviolet photoionization mass spectrometric study of ethylenediamine [J]. *Journal of Physical Chemistry A*, 2006, **110**(29): 9089-9098.

[24] BANIK S, SHUKLA A K, BARMAN S R. Optimal operating conditions and characteristics of acetone / CaF[sub 2] detector for inverse photoemission spectroscopy [J]. *Review of Scientific Instruments*, 2005, **76**(6): 066102.